J Physiol 596.15 (2018) pp 3271–3283

The Journal of Physiology

Hypercapnia-induced active expiration increases in sleep and enhances ventilation in unanaesthetized rats

Isabela P. Leirão, Carlos A. Silva Jr, Luciane H. Gargaglioni and Glauber S. F. da Silva

Department of Animal Morphology and Physiology, College of Agricultural and Veterinary Sciences, São Paulo State University (FCAV-UNESP), Jaboticabal, SP, Brazil

Key points

- Expiratory muscles (abdominal and thoracic) can be recruited when respiratory drive increases under conditions of increased respiratory demand such as hypercapnia.
- Studying hypercapnia-induced active expiration in unanaesthetized rats importantly contributes to the understanding of how the control system is integrated *in vivo* in freely moving animals.
- In unanaesthetized rats, hypercapnia-induced active expiration was not always recruited either in wakefulness or in sleep, suggesting that additional factors influence the recruitment of active expiration.
- The pattern of abdominal muscle recruitment varied in a state-dependent manner with active expiration being more predominant in the sleep state than in quiet wakefulness.
- Pulmonary ventilation was enhanced in periods with active expiration compared to periods without it.

Abstract Expiration is passive at rest but becomes active through recruitment of abdominal muscles under increased respiratory drive. Hypercapnia-induced active expiration has not been well explored in unanaesthetized rats. We hypothesized that (i) CO_2-evoked active expiration is recruited in a state-dependent manner, i.e. differently in sleep or wakefulness, and (ii) recruitment of active expiration enhances ventilation, hence having an important functional role in meeting metabolic demand. To test these hypotheses, Wistar rats (280–330 g) were implanted with electrodes for EEG and electromyography EMG of the neck, diaphragm (DIA) and abdominal (ABD) muscles. Active expiratory events were considered as rhythmic ABD_{EMG} activity interposed to DIA_{EMG}. Animals were exposed to room air followed by hypercapnia (7% CO_2) with EEG, EMG and ventilation ($\dot{V}_E$) recorded throughout the experimental protocol. No active expiration was observed during room air exposure. During hypercapnia, CO_2-evoked active expiration was predominantly recruited during non-rapid eye movement sleep. Its increased occurrence during sleep was evidenced by the decreased DIA-to-ADB ratio (1:1 ratio means that each DIA event is followed by an ABD event, indicating a high occurrence of ABD activity). Moreover, $\dot{V}_E$ was also enhanced ($P < 0.05$) in periods with active expiration. $\dot{V}_E$ had a positive correlation ($P < 0.05$) with the peak amplitude of ABD_{EMG} activity. The data demonstrate strongly that hypercapnia-induced active expiration increases during sleep and provides an important functional role to support $\dot{V}_E$ in conditions of increased respiratory demand.

(Received 4 June 2017; accepted after revision 1 August 2017; first published online 3 August 2017)

Corresponding author G. S. F. da Silva: Departamento de Morfologia e Fisiologia Animal, Faculdade de Ciências Agrárias e Veterinárias, Universidade Estadual Paulista Júlio de Mesquita Filho, Via de acesso Paulo Donato Castellane s/n, 14870-000, Jaboticabal, SP, Brazil. Email: glauber@ymail.com

I. P. Leirão and C. A. Silva contributed equally to this study.

DOI: 10.1113/JP274726

Abbreviations ABD_{EMG}, abdominal EMG; DIA_{EMG} and ABD_{EMG}, diaphragm and abdominal EMG; $\int DIA_{EMG}$ and $\int ABD_{EMG}$, integrated DIA_{EMG} and ABD_{EMG}; $Neck_{EMG}$, neck muscle EMG; NREM, non-rapid eye movement sleep; OSA, obstructive sleep apnoea; Peak Amp, peak amplitude; pFRG, parafacial respiratory group; REM, rapid eye movement; RF, respiratory frequency; RTN, retrotrapezoid nucleus; T_E, expiratory time; $\dot{V}_E$, ventilation; T_I, inspiratory time; T_{TOT}, total cycle duration; V_T, tidal volume; V_T/T_I, mean inspiratory flow.

Introduction

Respiration is a rhythmic process initiated spontaneously in the brainstem respiratory network. Under resting conditions expiration is passive, but expiratory muscles (abdominal and thoracic) can be recruited when respiratory drive increases under conditions such as hypercapnia, hypoxia or exercise (Iscoe, 1998; Iizuka, 2011; Feldman *et al.* 2013; Jenkin & Milsom, 2014). Recent evidence indicates that the parafacial respiratory group (pFRG), which overlaps to some extent with the retrotrapezoid nucleus (RTN), is a crucial brainstem site for generating active expiration (Janczewski *et al.* 2002; Mellen *et al.* 2003; Janczewski & Feldman, 2006; Huckstepp *et al.* 2015, 2016). Disinhibition of pFRG neurons and stimulation of the RTN/pFRG elicit active expiration in anaesthetized adult rats (Pagliardini *et al.* 2011), and the expiratory activity induced by hypercapnia is eliminated after chemical inhibition of the RTN/pFRG in *in situ* preparations (Abdala *et al.* 2009). This has led to the suggestion that the pre-Bötzinger complex generates the inspiratory rhythm, while the pFRG generates the expiratory rhythm, and each functions as distinct, but coupled, oscillators (Huckstepp *et al.* 2016).

The central respiratory control system is strongly influenced by vigilance state (Nattie, 2001; Feldman *et al.* 2003; Kuwaki *et al.* 2010; Nattie & Li, 2010; Pagliardini *et al.* 2012). Burke *et al.* (2015) recently reported that hypercapnic ventilatory response is highly dependent on vigilance state in rats. Moreover, the activity of most respiratory muscles is reduced in sleep [rapid eye movement (REM) and non-REM (NREM) sleep] (Sherrey & Megirian, 1977, 1980). The main inspiratory muscle, the diaphragm, is less affected but other accessory muscles exhibiting respiratory activity, such as the genioglossus, are strongly affected (Horner *et al.* 2002; Horner, 2008; Pagliardini *et al.* 2012). Interestingly, however, under eupnoeic conditions, where active expiration is absent normally, abdominal activity emerges in the REM-like sleep state in urethane-anaesthetized rats as well as in REM sleep, providing stability to breathing (Pagliardini *et al.* 2012; Andrews & Pagliardini, 2015). Evidence of hypercapnia-induced expiratory abdominal activity in rats extends from *in situ* preparations (Abdala *et al.* 2009; de Britto & Moraes, 2016; Jenkin *et al.* 2017) to *in vivo* anaesthetized animals (Iizuka & Fregosi, 2007; Lemes & Zoccal, 2014), but whether active expiration occurs in unanaesthetized animals under hypercapnic conditions in a state-dependent manner, i.e. differently in sleep and wakefulness, remains to be seen. Finally, active expiration has also been hypothesized to enhance ventilation by producing a more effective breathing pattern. In this context, the impact of hypercapnia-induced abdominal expiratory activity on the functional aspects of ventilation across vigilance states has been poorly explored. The characterization of CO_2-induced active expiration in unanaesthetized animals may advance our understanding of a rhythmic respiratory-related behaviour in freely moving animals that is essential to organismic homeostasis by enhancing sustained ventilation in conditions of increased respiratory demand.

Here we characterized active expiration in unanaesthetized, adult Wistar rats during hypercapnia in sleep and wakefulness. Moreover, we evaluated the functional impact of active expiration on the breathing pattern (balance of tidal volume and breathing frequency) in freely moving rats. To do so, combined measurements of EEG, EMG and ventilation (V_E) were performed in unanaesthetized, freely moving adult rats. Our data support the view that hypercapnia-induced active expiration occurs in a state-dependent manner (in wakefulness and more so in NREM sleep) and improves pulmonary ventilation when recruited.

Methods

Ethical approval and animals

Animal handling and experimental protocols were carried out in compliance with the guidelines of the National Council for Animal Care (CONCEA: Conselho Nacional de Controle de Experimentação Animal) and approved by the local Animal Care and Use Committee (Protocol no. 019289/14) of Sao Paulo State University (UNESP/FCAV). Animals (adult male Wistar rats; 280–330 g) were provided by the animal facility of UNESP (Botucatu campus), and, after transportation to the Jaboticabal campus of UNESP, they were acclimatized to the animal facility for at least 7 days before any procedures were done. Animals were housed under a 12 h dark–light cycle (lights on at 07.00 h) and had free access to water and food. All experiments were performed in the light phase between 09.00 and 16.00 h at room temperature 24–25°C.

Surgical procedures

Electrodes for EMG and EEG recordings were implanted surgically. Bipolar intramuscular EMG electrodes were

made of multi-strand, coated stainless steel wire (A-M Systems, Sequim, WA, USA) and EEG screw electrodes were commercially acquired (Plastics One Inc., Roanoke, VA, USA). Animals were anaesthetized with ketamine (100 mg kg^{-1}; I.P.) and xylazine (15 mg kg^{-1}; I.P.) to have the EMG and EEG electrodes implanted. For the insertion of EMG electrodes in the diaphragm (DIA_{EMG}) and abdominal (ABD_{EMG}) muscles, animals were placed in the supine position, and after local asepsis, a small horizontal incision was made in the lateral portion of the abdomen. For the ABD_{EMG}, the oblique abdominal muscle was targeted and a pair of electrodes were inserted. On the opposite side, for the DIA_{EMG}, a diagonal incision was made at the superior–lateral portion of the abdomen (from lateral to midline direction), following the ribcage border, from where the diaphragm muscle was accessed and electrodes were inserted. EMG electrode wires were tunnelled under the skin, and attached to an electrical socket secured between the animal's shoulder blades. For implanting the EEG electrodes and EMG electrodes in the neck muscle ($Neck_{EMG}$), the head and dorsal region of the neck were shaved and animals were placed in a stereotaxic apparatus. Next, the local asepsis was performed (dorsal region of the neck and head) followed by a subcutaneous injection of local anaesthetic (3% lidocaine hydrochloride). A skin midline incision was performed and the skull exposed. Three EEG electrodes were then screwed into the skull (Nattie & Li, 2002; da Silva *et al.* 2010), as follows: (i) the frontal electrode was placed 2 mm anterior to the bregma and 2 mm lateral to the midline (right side), (ii) the parietal electrode was placed 4 mm anterior to lambda and 2 mm lateral to the midline (right side) and (iii) the ground electrode was placed between the frontal and parietal electrodes (on the left), forming a triangle. A pair of electrodes was inserted into the dorsal cervical neck muscle to record the $Neck_{EMG}$. A plastic pedestal was used as an electrical socket and covered with a dust cap (Plastics One Inc.). The electrodes were mounted and fixed to the skull using acrylic resin. After surgery, the animals receive injections of antibiotic (enrofloxacin, Baytril; 10 mg kg^{-1} S.C., Bayer S.A., S.o Paulo, SP, Brazil) and analgesic (Flunixina Meglumina, Banamine; 2.5 mg kg^{-1} S.C., Schering-Plough, Kenilworth, NJ, USA)

Physiological recordings

For recordings, an insulated and shielded cable was connected to the plugs/sockets on the animal's head and neck. The cable was attached to an electrical swivel, which permitted free movement of the animal. A custom-made lid for the experimental chamber contained a hole through which the swivel was inserted and attached. From the swivel in the chamber lid a cable was connected to a four-channel amplifier (A-M Systems, model 1700). Signals were amplified (1000×), with 60 Hz notch filters, and band-pass filtered (low and high cut-off: 10 and 1000 Hz for EMG signals and 0.1 and 100 Hz for EEG signals, respectively). Signals were acquired (sample rate: 1 kHz) on a PowerLab (ADInstruments, Bella Vista, NSW, Australia) acquisition system and recorded using LabChart8 software. Online digital filtering was applied when necessary.

Ventilation ($\dot{V}_E$) was obtained by using a well-established barometric method (whole body plesthymography; for a detailed description see: Nattie & Li, 2002; da Silva *et al.* 2010, 2011, 2013). Briefly, before connecting the EEG and EMG wires, unanaesthetized rats were placed in the recording chamber and allowed to move freely (∼30 min) while the chamber was flushed with humidified air (1500 ml min^{-1}). The inflow gas was controlled using a gas-mixing pump. The flow rate through the animal chamber was maintained at 1500 ml min^{-1}. The temperature inside the chamber was continuously monitored. The breathing-related pressure oscillations were detected by a differential pressure transducer and amplified (MLT141 spirometer, Power Lab, ADInstruments). A volume calibration was performed by injecting a known air volume (1 ml) inside the chamber. Tidal volume (V_T) was calculated using the formula described by Drorbaug & Fenn (1955) and Bartlett & Tenney (1970). $\dot{V}_E$ was calculated as the product of V_T and respiratory frequency (RF). From the $\dot{V}_E$ trace, the inspiratory and expiratory time (T_I and T_E), total respiratory cycle duration (T_{TOT}) and the mean inspiratory flow (V_T/T_I) were calculated.

Experimental protocol

Experiments were performed a minimum of 8 days after the surgical procedures. All experiments began at 09.00 h (light phase) and were carried out at room temperature (24–25°C). Animals were placed in a cylindrical plethysmograph chamber (5 litres) and allowed to acclimatize for 30 min before connecting EEG and EMG wires. During this period the chamber was flushed with room air at a flow rate of 1500 ml min^{-1}. Then, small wires for recording EMG and EEG signals were connected to the implanted wires in the animal and connected to an electrical swivel in the internal face of the lid, and from the external face of the lid to the amplifiers (A-M Systems, model 1700). The use of a swivel was critical to keep the animal undisturbed and the wires untangled throughout the experimental protocol, and this wire arrangement allowed the animal to move freely inside the chamber. With all cables in place, further time (∼30 min) was given before starting to record signals. Room air was continuously flushed during the whole period of adaption. After that, EEG and EMG signals were recorded during room air exposure for a time interval of usually 40–60 min that yielded recording signals in different sleep–wake cycles.

The gas was then switched to a hypercarbic gas mixture (7% CO_2, 21% O_2, N_2 balance) provided by a gas mixing system (GSM-3 Gas Mixer; CWE Inc., Ardmore, PA, USA) at a flow rate of 1500 ml min^{-1}. Animals were exposed to hypercapnia for 60 min, and physiological parameters described above were measured throughout the time of exposure. After the experiments all animals were killed with an overdose of anaesthesia.

Data and statistical analyses

Data were collected electronically for subsequent analyses. The following criteria were applied for data analysis: all periods containing artifacts of animals' movements, exploratory behaviours and grooming were excluded from analysis, whereas periods of quiet wakefulness and sleep were all analysed. EEG and $Neck_{EMG}$ recordings were used to define sleep or wakefulness states (Nattie & Li, 2002; da Silva *et al.* 2010). The EMGs from respiratory muscles were integrated (0.05 s), and the muscle activity was calculated as the peak amplitude (Peak Amp) of the integrated DIA_{EMG} ($\int DIA_{EMG}$) and ABD_{EMG} ($\int ABD_{EMG}$), respectively. Event detection and Peak Amp analysis were performed on Clampfit software on a peak-to-peak basis during different alert states (sleep and wakefulness). The detection and selection of $\int DIA_{EMG}$ and $\int ABD_{EMG}$ during the data analysis were all performed within the exact time window for each signal. This allowed the assessment of DIA-to-ABD ratio within a given time window of the trace. This ratio expresses the occurrence of ABD events in relation to the DIA. A 1:1 ratio indicates a high occurrence of ABD activity (each DIA event is followed by an ABD event). Hence, the lower the ratio, the higher the occurrence of active expiration. All data were exported and further processed in an Excel spreadsheet where the $\int DIA_{EMG}$ and $\int ABD_{EMG}$ data were normalized to their largest integrated ($\int$) EMG Peak Amp obtained during the wakefulness state for each muscle. The normalized Peak Amp values were used for comparisons. For the purpose of analysis, active expiration was defined by the presence of ABD_{EMG} expiratory activity, i.e. rhythmic burst of ABD_{EMG} activity (between inspiratory DIA_{EMG} bursts) above tonic levels (Pagliardini *et al.* 2011; Huckstepp *et al.* 2015). Data were analysed in a state-dependent manner, separated into two states – quiet wakefulness and non-REM sleep – both observed consistently throughout the experimental protocol both during room air and hypercapnia exposures. REM sleep periods were very short and in most of the experiments were not present. Hence, all analysis during sleep is reported for NREM sleep. Arousal states were determined based on EEG and neck EMG and categorized as previously described (Nattie & Li, 2001, 2002; Taylor *et al.* 2006; da Silva *et al.* 2010). All active expiration events (according to the criteria) in each animal data set were averaged. Distributions (histograms) of the $\int ABD_{EMG}$ Peak Amp (absolute number of events) were determined individually for each rat in different states during hypercapnia, and these data were also reported in box plots. For ventilatory variables, the analyses during hypercapnia were run in periods with or without active expiration in a state-dependent manner. Data were expressed as mean ± SEM. Student's *t* tests and two-way ANOVA for repeated measures followed by *post hoc* tests were performed accordingly. A Pearson test was used for correlation analysis. P was set at 0.05 to indicate a significant difference.

Results

Room air

EEG and $Neck_{EMG}$ recordings allowed identification of sleep–wake states. Figure 1*A* shows a representative spectrogram, EEG and $Neck_{EMG}$ (top, middle and bottom, respectively) of an animal during room air and hypercapnia exposure. During room air exposure, the percentage of time spent in wakefulness or in NREM sleep in the group data averaged 33.7 and 63.3%, respectively. Figure 1*B* and *C* depict the recorded physiological variables during room air exposure in both wakefulness and sleep. The mean breathing frequency measured by $\int DIA_{EMG}$ events was 101 ± 5 and 86 ± 4 cycles min^{-1} in wakefulness and sleep ($n = 8$), respectively. As for the ABD_{EMG} activity, regardless of the state, no active expiration was observed during room air exposure ($n = 8$), i.e. no rhythmic expiratory ABD_{EMG} activity was present, either in wakefulness (Fig. 1*B*) or in sleep (Fig. 1*C*). The absence of active expiration was consistent among animals breathing room air.

Hypercapnia exposure

During hypercapnia exposure (7% CO_2) the percentage of time in wakefulness or in NREM sleep averaged 55.8 and 44.5%, respectively. The hypercapnia-induced decrease in sleep time was the result of a longer time spent in wakefulness. These effects of hypercapnia in the arousal state have been well documented in the literature (Taylor *et al.* 2006; Buchanan & Richerson, 2010; Dias *et al.* 2010; Buchanan *et al.* 2015; Vicente *et al.* 2016). The recruitment of abdominal muscles occurred during exposure to CO_2 (Fig. 1*D*–*G*). Hypercapnia-induced active expiration was not present during the entire period of CO_2 exposure. Figure 1*D* is an example showing that during hypercapnia in a wakefulness period active expiration was not present initially, but that expiratory ABD_{EMG} activity emerged after a brief period of movement. The $\int ABD_{EMG}$ Peak Amp associated with abdominal expiratory activity during wakefulness was relatively constant (Fig. 1*F*). During sleeping periods, however, active expiration was more consistent, and the $\int ABD_{EMG}$ Peak Amp associated with

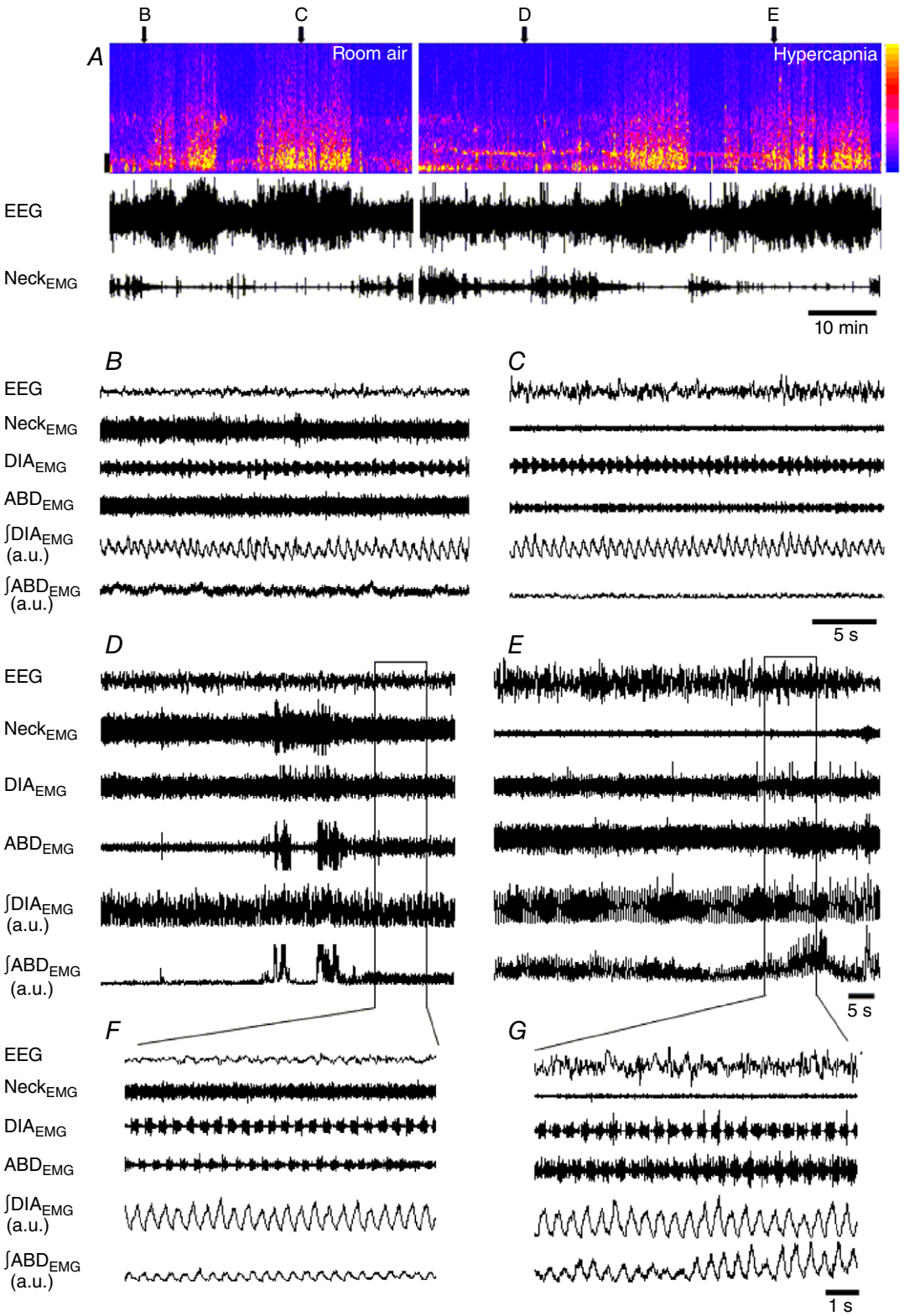

Figure 1. State-dependent activity of abdominal and diaphragm activity during room air and hypercapnia exposure
A, EEG spectrogram, EEG and Neck$_{EMG}$ raw recordings (top, middle and bottom, respectively) of a representative animal during a typical experimental protocol in room air (left) and hypercapnia exposure (right). In the EEG spectrogram, the colour intensity, as indicated by the colour calibration bar to the right side, corresponds to the amount of signal power at a given time and frequency. On the left side, frequency calibration bar: 2 Hz. Note that

the animal cycles between wake and sleep in both conditions: room air and hypercapnia. Above the spectrogram, the letters and arrows indicate for each of the respective panels where their traces were withdrawn and expanded. The expanded EEG and EMGs [raw and integrated abdominal ($\int ABD_{EMG}$) and diaphragm ($\int DIA_{EMG}$) signals] during room air are shown in periods of wakefulness (*B*) and sleep (*C*), and during hypercapnia in wakefulness (*D*) and sleep (*E*). The horizontal rectangles in *D* and *E* depict the expanded trace shown in *F* and *G*, respectively. Note the absence of active expiration during room air (*B* and *C*) and its recruitment during hypercapnia (*D*–*G*). [Colour figure can be viewed at wileyonlinelibrary.com]

expiratory ABD_{EMG} activity was often highly variable (Fig. 1*E* and *G*). This general pattern was also observed in other animals (Figs 2 and 3). It is noteworthy that 1 out of 9 rats recorded in the present study did not show any active expiration while awake, but only while sleeping.

Figure 2 illustrates the group data (box plot) and the distribution (histograms) of $\int ABD_{EMG}$ Peak Amp (i.e. active expiration events) for each individual animal in different states. The box plot (Fig. 2, top) shows an apparent larger variability of $\int ABD_{EMG}$ data during sleep. The greater variability during sleep is confirmed by the coefficient of variation (CV) of $\int ABD_{EMG}$ Peak Amp, which was 96.4 and 65% during sleep and wakefulness, respectively. The $\int DIA_{EMG}$ had lower variability compared to abdominal activity and was not influenced by vigilance state (the CV of $\int$DIAEMG was 35.5 and 28.8% during sleep and quiet wakefulness, respectively). Moreover, the histograms demonstrate that, for most animals, the number of events of active expiration as well as the number of a given $\int ABD_{EMG}$ Peak Amp tended to be greater during sleep (right column, Fig. 2) when compared to wakefulness (left column, Fig. 2).

The DIA-to-ADB ratio, $\int ABD_{EMG}$ Peak Amp, $\int DIA_{EMG}$ Peak Amp and breathing frequency during hypercapnia are presented in Fig. 3. The increased occurrence of active expiration during sleep is evidenced by the decreased DIA-to-ADB ratio (a 1:1 ratio means that each DIA is followed by an ABD event, indicating a high occurrence of ABD activity). Figure 3*A* shows that this ratio decreased during sleep (∼2:1) compared to wakefulness (∼7:1) (mean values: 1.92 ± 0.2 *vs.* 6.87 ± 3; wakefulness and sleep, respectively; $P = 0.02$, $n = 8$). In Fig. 3*B*, the amplitude of $\int ABD_{EMG}$ was 33.2% larger during sleep when compared to wakefulness (0.205 ± 0.02 *vs.* 0.307 ± 0.05; $P = 0.06$, $n = 8$; normalized Peak Amp for wakefulness and sleep, respectively) (Fig. 3*B*). Breathing frequency had a ∼6% reduction (147 ± 5 *vs.* 138 ± 2 cycles min^{-1}, $P = 0.066$, $n = 8$) and $\int DIA_{EMG}$ Peak Amp (0.43 ± 0.4 *vs.* 0.45 ± 0.06, $n = 8$) was not different between wakefulness and sleep, respectively (Fig. 3*C* and *D*).

Active expiration and assessment of ventilatory variables

Hypercapnia consistently recruited active expiration, but periods in which active expiration failed to occur were also observed (Fig. 1). To assess the functional role of active expiration during hypercapnia in unanaesthetized freely moving rats, ventilatory measurements were recorded along with EEG and $Neck_{EMG}$, DIA_{EMG} and ABD_{EMG}. First, ventilatory variables were assessed in the trace periods with active expiration and compared to the same variables in periods without active expiration. Figure 4 shows the relative change of the ventilatory variables analysed separately in periods with or without active expiration. The ventilatory response to hypercapnia was enhanced by active expiration. V_T, RF and $\dot{V}_E$ were higher ($P = 0.04$, $P = 0.026$, $P = 0.003$, $n = 7$; respectively) when active expiration was present, and this effect was not dependent on sleep–wake cycle. T_I was not significantly affected by the presence of active expiration, whereas T_E and T_{TOT} decreased ($P = 0.02$ and $P = 0.011$, respectively) in periods where active expiration was present. Therefore, in unanaesthetized rats during hypercapnia, whenever present, active expiration enhanced $\dot{V}_E$ through both increased V_T and RF; the reduction in T_{TOT} was mainly achieved by a diminished T_E. These effects were independent of vigilance state.

Figure 5 shows a representative trace of EEG, $Neck_{EMG}$, DIA_{EMG} and ABD_{EMG} recorded across a sleep–wake cycle during hypercapnia. Note that during the natural transition from sleep to wakefulness there was increasing ABD_{EMG} activity (also seen in Fig. 1*E* and *G*) within the sleeping period, but ABD_{EMG} rhythmic activity ceased completely as soon as the animal woke up. As mentioned earlier, the $\int ABD_{EMG}$ Peak Amp associated with abdominal expiratory activity during wakefulness was relatively constant (see Fig. 1*F*), whereas this type of increasing $\int ABD_{EMG}$ Peak Amp occurred more during sleep (see Figs 1*E* and *G* and 5).

The ventilatory variables were measured breath-by-breath over this recording to assess the overall functional impact of the increasing expiratory activity on $\dot{V}_E$. A breath-by-breath analysis was run by taking each breath and the corresponding $\int ABD_{EMG}$ Peak Amp (representative trace and scatter plots, Fig. 5). The $\int ABD_{EMG}$ Peak Amp was positively correlated with RF ($r = 0.56$, $P < 0.001$), $\dot{V}_E$ ($r = 0.37$, $P = 0.003$) and V_T/T_I ($r = 0.45$, $P < 0.001$) and negatively correlated with T_I ($r = -0.47$, $P < 0.001$), while no significant correlation was observed with T_E and V_T ($P = 0.5$ and $P = 0.11$, respectively). Therefore, once active expiration was present, the increasing ABD_{EMG} activity improved $\dot{V}_E$ through inspiratory actions, mainly due to increases

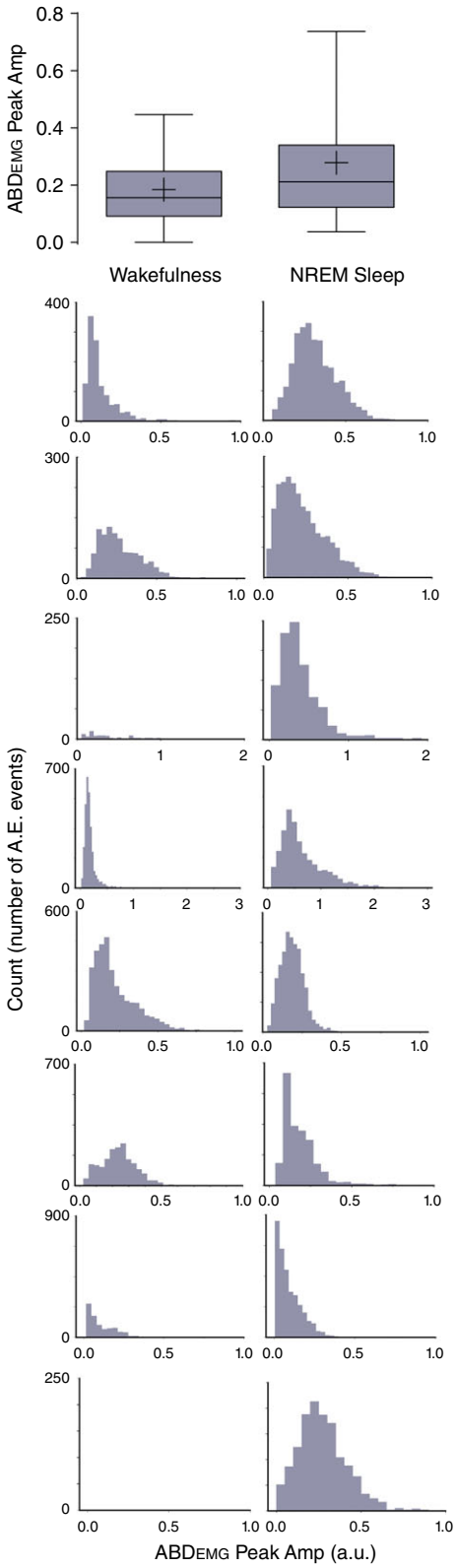

Figure 2. Distribution of active expiration (A.E.) events ($\int ABD_{EMG}$ Peak Amp) during hypercapnia in wakefulness and sleep
Top panel shows the group data as box plots in which the centre line shows the median; box limits indicate the 25th and 75th percentiles; whiskers extend to 5th and 95th percentiles; and crosses represent sample means. Each histogram (row) represents the distribution for one individual animal in both vigilance states: wakefulness (left column) and sleep (right column). Note that one animal (bottom row) did not present active expiration in wakefulness, but only in sleep. [Colour figure can be viewed at wileyonlinelibrary.com]

in RF (decrease T_I) and V_T [augmented mean inspiratory flow (V_T/T_I)].

Discussion

In the present study, while no active expiration was observed in unanaesthetized animals breathing room air (regardless of sleep–wake state), abdominal muscle expiratory activity was recruited during hypercapnia exposure with an increased occurrence during NREM sleep compared to wakefulness. Moreover, whenever present, active expiration was associated with an increase in $\dot{V}_E$ compared to periods without it.

Active expiration has gained attention recently arising from data indicating the existence of a brainstem conditional expiratory oscillator, the pFRG, distinct from (but coupled to) the inspiratory oscillator, the pre-Bötzinger complex (Pagliardini *et al.* 2011; Huckstepp *et al.* 2015, 2016). Under eupnoeic conditions (rats breathing room air), urethane-anaesthetized rats increased abdominal activity switching from tonic to expiratory rhythmic activity (i.e. active expiration) with the transition from NREM to REM-like sleep (Pagliardini *et al.* 2012). This has also been reported to occur during natural REM sleep in unanaesthetized rats (Andrews & Pagliardini, 2015). In the present study, we did not observe active expiration (expiratory ABD_{EMG} activity) during sleep in animals breathing room air. The source of this difference is not clear. However, in the urethane-anaesthetized rats, in ∼46% of recordings (6 out of 13) ABD_{EMG} activity was tonic (no active expiration) and did not change across sleep–wake cycle (Pagliardini *et al.* 2012). Likewise, in unanaesthetized rats in room air, events of active expiration (that lasted for more than three consecutive breaths as defined by the authors) occurred in only ∼49% of REM epochs (147 out of 300 REM epochs) (Andrews & Pagliardini, 2015). The amount of REM sleep seen in our study was small, suggesting that long-lasting recording experiments are needed to yield sufficient REM episodes to accurately examine the recurrent activation of ABD_{EMG} activity.

In the present study, abdominal oblique muscles were targeted as representative of hypercapnia-induced expiratory abdominal activity. Abdominal muscles are innervated by branches from the ventral rami of intercostal nerves of thoracic segments and from lumbar segments, and there is a variable overlap of the abdominal

motoneurons in regions of the ventral horn (Iscoe, 1998). The rectus abdominis has little or no respiratory-related activity in humans and conscious rats (Abe *et al.* 1996; Iscoe, 1998). In contrast, and in agreement with our data, a consistent response of the abdominal obliques to hypercapnia has been reported in both humans and rats (Jeffries *et al.* 1984; Takasaki *et al.* 1989; Abe *et al.* 1996; Iscoe, 1998; Iizuka, 2011; Pagliardini *et al.* 2012; Andrews & Pagliardini, 2015).

An increased respiratory drive leads to emergence of expiratory abdominal activity in humans (Badr *et al.* 1990; Wakai *et al.* 1992; Abe *et al.* 1996), dogs (Oliven *et al.* 1985; Smith *et al.* 1989, 1990) and rodents (Sherrey *et al.* 1988; Iizuka & Fregosi, 2007; Lemes & Zoccal, 2014). In rats, evidence of hypercapnia-induced expiratory ABD_{EMG} activity extends from *in situ* preparations (Abdala *et al.* 2009; de Britto & Moraes, 2016; Jenkin *et al.* 2017) to *in vivo* anaesthetized animals (Iizuka & Fregosi, 2007; Lemes & Zoccal, 2014). Fewer studies, however, have examined its occurrence in unanaesthetized rats in different vigilance states. In agreement with the literature, we reported that the CO_2 drive to breathe (hypercapnia exposure) recruits active expiration in unanaesthetized adult rats. Two observations are noteworthy: (i) in unanaesthetized rats, the expiratory ABD_{EMG} activity was not always recruited during exposure to hypercapnia either in wakefulness or in sleep, suggesting that other factors also influence the recruitment of active expiration; and (ii) the pattern of this recruitment varied in a state-dependent manner with active expiration being more predominant in NREM sleep state compared to quiet wakefulness.

The observation (i) that active expiration failed to be consistently recruited by hypercapnia in both sleeping and awake rats is consistent with the observation that active expiration was not consistently recruited in REM sleep (Andrews & Pagliardini, 2015). It seems that factors other than levels of chemical drive and state influence abdominal expiratory activity. Some evidence suggests that the posture of the animals may affect the activity of ABD_{EMG}. Although Sherrey *et al.* (1988) reported that hypercapnia elicited active expiration in rats regardless of posture, when the rat curled its body oppositely from the side of the recording electrodes, the ABD_{EMG} activity was large and decreased to a minimum when the rat was curled toward the electrodes. In humans, body position is also suggested to play a role in the emergence of active expiration, as the abdominal recruitment elicited by increased inspiratory resistance was seen in upright but not supine subjects (Martin & De Troyer, 1982; Badr *et al.* 1990). Moreover, De Troyer *et al.* (1989)

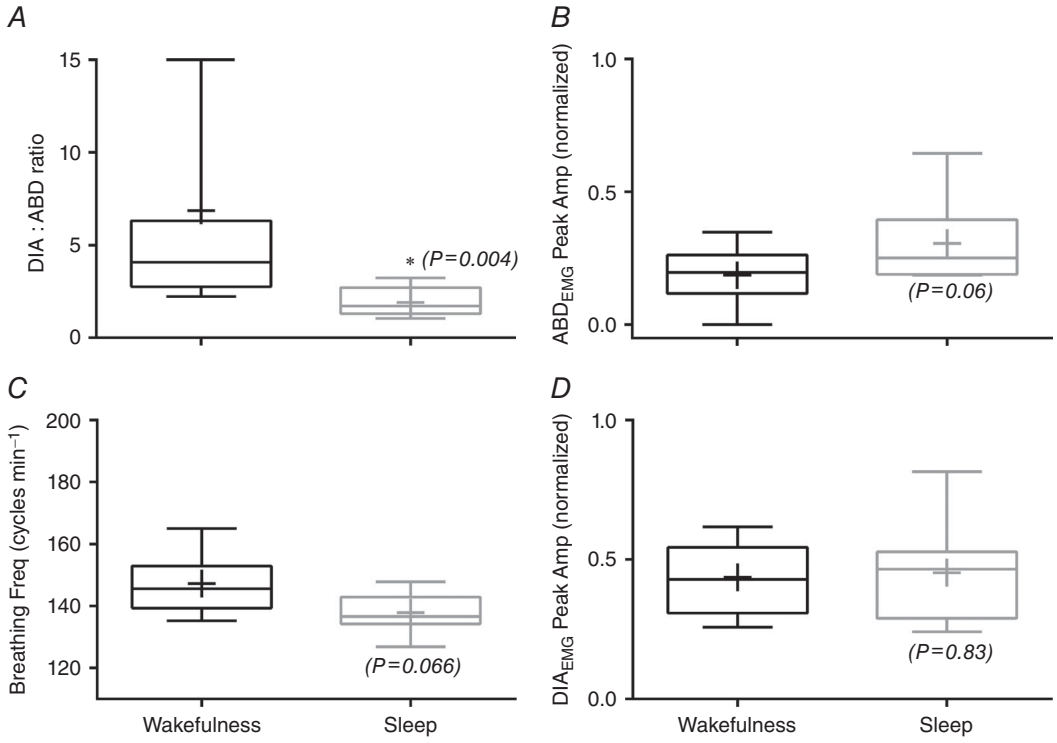

Figure 3. Respiratory muscle EMG and breathing frequency during hypercapnia in different vigilance states: wakefulness and sleep
Box plots: centre line shows the median; box limits indicate the 25th and 75th percentiles; whiskers extend to 5th and 95th percentiles; and crosses represent sample means. The panels show the DIA-to-ADB ratio (*A*), $\int ABD_{EMG}$ Peak Amp (*B*), breathing frequency (*C*) and $\int DIA_{EMG}$ Peak Amp (*D*) ($n = 8$). The *P* values are indicated for the sleep data set compared to wakefulness. *Difference ($P < 0.05$) of sleep state compared to wakefulness state.

suggested that, in conscious dogs, proprioceptive inputs from the abdominal wall could promote or modulate ABD activity during expiration. To our knowledge, how the proprioceptive components act to inhibit or facilitate the emergence of active expiration remains uncertain. It is worth mentioning that, in unanaesthetized, freely moving rats, active expiration seems to be a complex respiratory motor behaviour influenced by different components (i.e. chemical drive, state and proprioception); however, how these are computed in the brainstem expiratory generating network to finally express active expiration remains unknown.

The underlying mechanism of the second observation (ii), that active expiration is more predominant in NREM sleep, is also elusive. Recent evidence supports the role of neurons (different from the RTN Phox2b neurons) in the pFRG as the brainstem site that generates active expiration (Huckstepp *et al.* 2015, 2016). Burke *et al.* (2015) reported that RTN stimulation caused active expiration only when the rats were awake. In contrast, other reports in the literature showed that active expiration is recruited during sleep in rats and humans (Pagliardini *et al.* 2012; Andrews & Pagliardini, 2015; and in our present study). The fact that RTN neurons drive

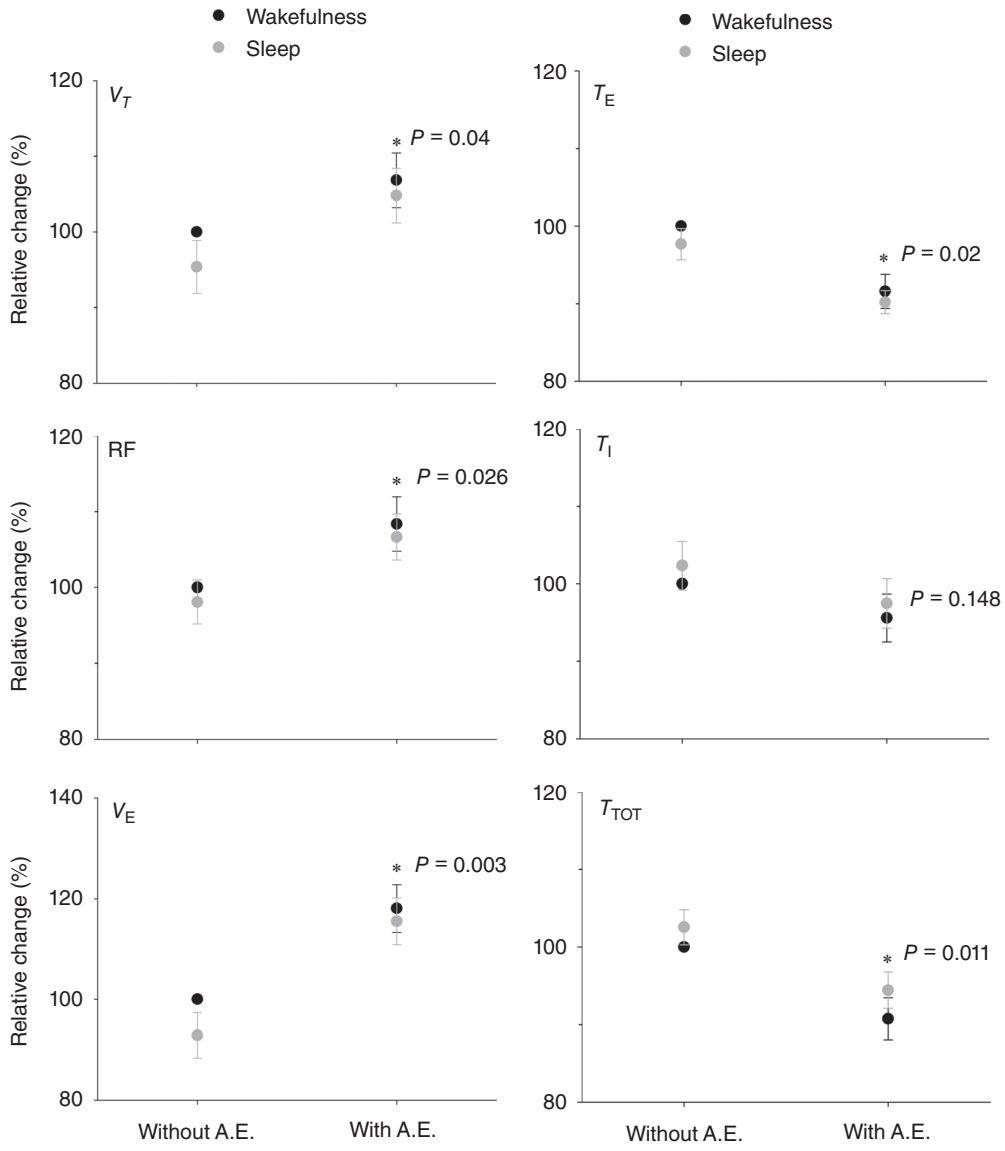

Figure 4. Comparison of ventilatory variables during hypercapnia in periods with or without recruitment of active expiration
V_T and T_E top panels, RF and T_I middle panels, and VE and T_{TOT} bottom panels. (∗) indicates difference ($P < 0.05$) comparing the ventilatory variables with and without active expiration (A.E.) ($n = 7$). The P values are indicated.

active expiration only during wakefulness suggests that different mechanisms to recruit active expiration may be involved during sleep. Alternatively, as suggested by Burke *et al.* active expiration could yet be triggered in NREM sleep by stimulating a larger fraction of RTN neurons. Serotoninergic (Lemes *et al.* 2016) and cholinergic (Boutin *et al.* 2017) neurotransmission in the RTN/pFRG have now been reported to induce active expiration in anaesthetized rats. Disinhibition of these neurons has been shown to underlie the recruitment of active expiration (Pagliardini *et al.* 2011) and it is quite possible that this disinhibition is influenced by vigilance state. The modulation of

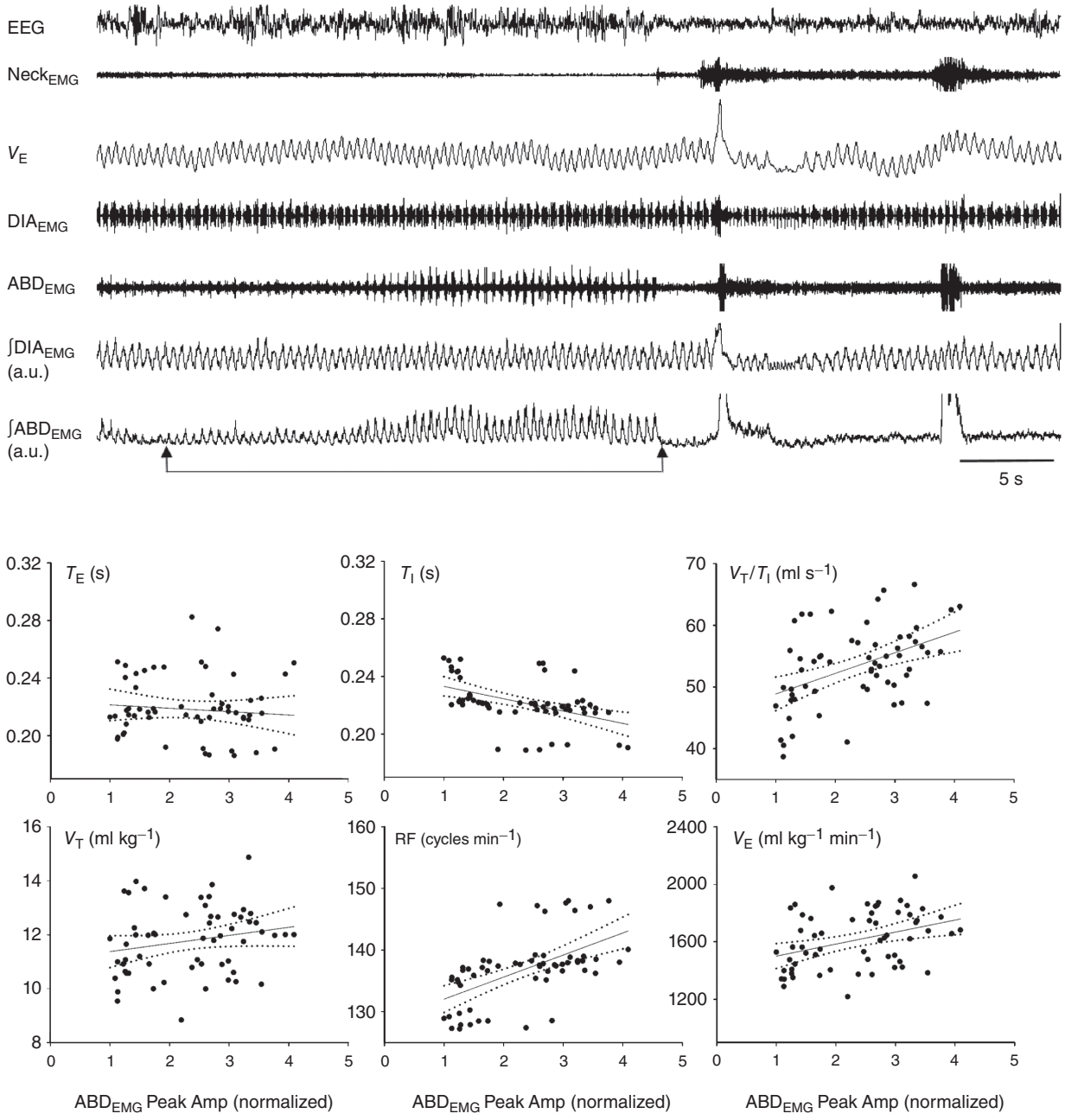

Figure 5. Functional impact of active expiration with increasing ABD$_{EMG}$ activity on ventilatory variables during hypercapnia
Top traces depict EEG, Neck$_{EMG}$, barometric V_E recording and raw and integrated DIA$_{EMG}$ and ABD$_{EMG}$. Two arrows below the ∫ABD$_{EMG}$ trace show the interval time with increasing ABD$_{EMG}$ activity from which correlation analyses between active expiration (∫ABD$_{EMG}$ Peak Amp) and ventilation were performed. A breath-by-breath analysis was run in 60 events. Scatter plots show the correlation between increasing ∫ABD$_{EMG}$ Peak Amp and T_E, T_I and V_T/T_I (top row) and V_T, RF and V_E (bottom row).

pFRG neurons across state as well as the state-dependent involvement of neurotransmitters is currently not well known. It has also been hypothesized that the activity of different brainstem CO_2 chemoreceptor sites varies in a state-dependent manner (Nattie, 2000; da Silva *et al.* 2010; Nattie & Li, 2010), and hence it is also possible that the different CO_2-sensitive cell types input into and modulate pFRG neurons to generate active expiration differently in sleep and wakefulness.

The state-dependent enhancement of CO_2-induced active expiration may also be related to a change in peripheral airway resistance. In humans during NREM sleep, expiratory abdominal muscles are recruited by sustained inspiratory resistive loading (Badr *et al.* 1990; Henke *et al.* 1991), obstructive sleep apnoea (Jeffries *et al.* 1984; Praud *et al.* 1989) and acute bronchospasm in asthmatics (Issa & Sullivan, 1985), and an interaction of increased airway resistance and chemoreceptor stimuli have been suggested as necessary to recruit abdominal muscles during NREM sleep (Badr *et al.* 1990; Henke *et al.* 1992). This suggestion emphasizes the importance of studying active expiration in hypercapnic conditions. In rodents, it has been shown that the activity of airway muscles such as the cricothyroid, nasolabial (Sherrey & Megirian, 1977) and genioglossal muscles (Horner, 2008) changes across state, which implies changes in airway resistance. In the present study, we did not record from other airway respiratory muscles, but it remains possible that the increase in ABD_{EMG} activity during NREM sleep (Fig. 1*E* and *F*) was related to fluctuation of airway resistance during sleep.

Another important aspect of the present study is the description of the functional impact of active expiration on the ventilatory variables. We demonstrate here that, regardless of vigilance state, the presence of active expiration elicited an enhancement of ventilation achieved by increases in both V_T and RF (with decrease in T_E and T_{TOT}; Fig. 4). This is in agreement with the notion that active expiration can increase V_T by recruiting the expiratory reserve volume and increase RF by shortening the expiratory time constant (shorter than the passive time constant of the system) with a decreased T_E and T_{TOT} (Jenkin & Milsom, 2014). In humans, the main mechanical consequence of abdominal recruitment, specifically during sustained respiratory loading, was a shortened T_E and increased RF (Badr *et al.* 1990; Henke *et al.* 1991).

When active expiration was already present and the ABD_{EMG} activity was recruited further in a progressive manner, this was achieved mainly by an increase in RF (i.e. with diminished T_I) and increased mean inspiratory flow (V_T/T_I), although inspiratory DIA_{EMG} activity did not increase to support the increased V_T/T_I. The lack of further change in V_T could reflect maximum recruitment of the expiratory reserve volume. At this point further recruitment of the expiratory muscles can only serve to produce complete exhalation within the same T_E. Associated with this may be changes in compliance or resistance (lengthening tau, the passive time constant) reflecting state-dependent changes in airway muscle activity (and hence resistance). Also, ABD_{EMG} activity could place the diaphragm at a better length for generating tension and improving mechanical output during inspiration. Indeed, these mechanical consequences of expiratory muscle recruitment have been reported during transient events in sleeping humans (Henke *et al.* 1991, 1992). The observed effect of increasing ABD_{EMG} activity on inspiration (increased V_T/T_I and decreased T_I) could also be associated with a parallel increase in activity of other inspiratory accessory muscles that were not recorded in the present study.

The respiratory control system is dedicated to maintaining the rhythmic activity of respiratory muscles via respiratory motor output in a coordinated fashion. Their rhythmic activities have to ultimately match metabolic demand and maintain organismic homeostasis of blood gases. Using a simple, yet elegant approach, the present study brings fundamental knowledge about control of breathing through the following integrative perspectives on active expiration: the brainstem expiratory generating network, which is influenced by sleep state (although the underlying mechanisms remain to be further explored), and, simultaneously, active expiration enables optimal ventilatory strategies during ventilatory challenge, further supporting important physiological function. By showing the state dependence of the hypercapnia-induced active expiration, we also have another (patho)physiological aspect. The hypercapnia exposure used in the present study elicits a ∼15 mmHg rise in arterial P_{CO_2}, reaching values of about 50 mmHg (for detailed values see da Silva *et al.* 2011). A rise in blood CO_2 can be life threatening, and hypercapnia is a significant factor in diseases such as obstructive sleep apnoeas (OSAs) with consequent variable degrees of morbidity (and mortality). For example, an increased occurrence of active expiration during sleep was reported in patients with OSA, compared to subjects without OSA (Jeffries *et al.* 1984). Hypercapnia was present in patients with OSA and some of them who had significant blood gas abnormalities, i.e. P_{CO_2} values above 50 mmHg, presented the highest ABD expiratory activity during sleep (Jeffries *et al.* 1984). Therefore, appropriate respiratory motor outputs as well as ventilatory adjustments to hypercapnia are highly desired.

In conclusion, the present study in unanaesthetized adult rats indicates that while no active expiration is present under normocapnic conditions in any vigilance state, ABD_{EMG} expiratory activity is recruited during hypercapnia predominantly during NREM sleep. We also show that active expiration is associated with improved

ventilation achieved by both increased V_T and RF, with decreased T_E and T_{TOT}.

References

Abdala AP, Rybak IA, Smith JC & Paton JFR (2009). Abdominal expiratory activity in the rat brainstem–spinal cord *in situ*: patterns, origins and implications for respiratory rhythm generation. *J Physiol* **587**, 3539–3559.

Abe T, Kusuhara N, Yoshimura N, Tomita T & Easton PA (1996). Differential respiratory activity of four abdominal muscles in humans. *J Appl Physiol* **80**, 1379–1389.

Andrews CG & Pagliardini S (2015). Expiratory activation of abdominal muscle is associated with improved respiratory stability and an increase in minute ventilation in REM epochs of adult rats. *J Appl Physiol* **119**, 968–974.

Badr MS, Skatrud JB, Dempsey JA & Begle RL (1990). Effect of mechanical loading on expiratory and inspiratory muscle activity during NREM sleep. *J Appl Physiol* **68**, 1195–1202.

Bartlett D & Tenney SM (1970). Control of breathing in experimental anemia. *Respir Physiol* **10**, 384–395.

Boutin RCT, Alsahafi Z & Pagliardini S (2017). Cholinergic modulation of the parafacial respiratory group. *J Physiol* **595**, 1377–1392.

de Britto AA & Moraes DJA (2016). Non-chemosensitive parafacial neurons simultaneously regulate active expiration and airway patency under hypercapnia in rats. *J Physiol* **6**, 2043–2064.

Buchanan GF & Richerson GB (2010). Central serotonin neurons are required for arousal to CO_2. *Proc Natl Acad Sci USA* **107**, 16354–16359.

Buchanan GF, Smith HR, MacAskill A & Richerson GB (2015). 5-HT_{2A} receptor activation is necessary for CO_2-induced arousal. *J Neurophysiol* **114**, 233–243.

Burke PGR, Kanbar R, Basting TM, Hodges WM, Viar KE, Stornetta RL & Guyenet PG (2015). State-dependent control of breathing by the retrotrapezoid nucleus. *J Physiol* **593**, 2909–2926.

Dias MB, Li A & Nattie E (2010). The orexin receptor 1 (OX1R) in the rostral medullary raphe contributes to the hypercapnic chemoreflex in wakefulness, during the active period of the diurnal cycle. *Respir Physiol Neurobiol* **170**, 96–102.

Drorbaug JE & Fenn WO (1955). A barometric method for measuring ventilation in newborn infants. *Pediatrics* **16**, 81–87.

Feldman JL, Mitchell GS & Nattie EE (2003). Breathing: rhythmicity, plasticity, chemosensitivity. *Annu Rev Neurosci* **26**, 239–266.

Feldman JL, Del Negro CA & Gray PA (2013). Understanding the rhythm of breathing: so near, yet so far. *Annu Rev Physiol* **75**, 423–452.

Henke KG, Badr MS, Skatrud JB & Dempsey JA (1992). Load compensation and respiratory muscle function during sleep. *J Appl Physiol* **72**, 1221–1234.

Henke KG, Dempsey JA, Badr MS, Kowitz JM & Skatrud JB (1991). Effect of sleep-induced increases in upper airway resistance on respiratory muscle activity. *J Appl Physiol* **70**, 158–168.

Horner RL (2008). Neuromodulation of hypoglossal motoneurons during sleep. *Respir Physiol Neurobiol* **164**, 179–196.

Horner RL, Liu X, Gill H, Nolan P, Liu H & Sood S (2002). Effects of sleep–wake state on the genioglossus vs.diaphragm muscle response to CO_2 in rats. *J Appl Physiol* **92**, 878–887.

Huckstepp RTR, Cardoza KP, Henderson LE & Feldman JL (2015). Role of parafacial nuclei in control of breathing in adult rats. *J Neurosci* **35**, 1052–1067.

Huckstepp RTR, Henderson LE, Cardoza KP & Feldman JL (2016). Interactions between respiratory oscillators in adult rats. *Elife* **5**, 1–22.

Iizuka M (2011). Respiration-related control of abdominal motoneurons. *Respir Physiol Neurobiol* **179**, 80–88.

Iizuka M & Fregosi RF (2007). Influence of hypercapnic acidosis and hypoxia on abdominal expiratory nerve activity in the rat. *Respir Physiol Neurobiol* **157**, 196–205.

Iscoe S (1998). Control of abdominal muscles. *Prog Neurobiol* **56**, 433–506.

Issa FG & Sullivan CE (1985). Respiratory muscle activity and thoracoabdominal motion during acute episodes of asthma during sleep. *Am Rev Respir Dis* **132**, 999–1004.

Janczewski WA & Feldman JL (2006). Distinct rhythm generators for inspiration and expiration in the juvenile rat. *J Physiol* **570**, 407–420.

Janczewski WA, Onimaru H, Homma I & Feldman JL (2002). Opioid-resistant respiratory pathway from the preinspiratory neurones to abdominal muscles: *in vivo* and *in vitro* study in the newborn rat. *J Physiol* **545**, 1017–1026.

Jeffries B, Brouillette RT & Hunt CE (1984). Electromyographic study of some accessory muscles of respiration in children with obstructive sleep apnea. *Am Rev Respir Dis* **129**, 696–702.

Jenkin SEM & Milsom WK (2014). *Expiration: Breathing's other face*, 1st edn. Elsevier, Amsterdam. Available at: https://doi.org/10.1016/B978-0-444-63488-7.00008-2.

Jenkin SEM, Milsom WK & Zoccal DB (2017). The Kölliker–Fuse nucleus acts as a timekeeper for late-expiratory abdominal activity. *Neuroscience* **348**, 63–72.

Kuwaki T, Li A & Nattie E (2010). State-dependent central chemoreception: a role of orexin. *Respir Physiol Neurobiol* **173**, 223–229.

Lemes EV, Colombari E & Zoccal DB (2016). Generation of active expiration by serotoninergic mechanisms of the ventral medulla of rats. *J Appl Physiol* **121**, 1135–1144.

Lemes EV & Zoccal DB (2014). Vagal afferent control of abdominal expiratory activity in response to hypoxia and hypercapnia in rats. *Respir Physiol Neurobiol* **203**, 90–97.

Martin JG & De Troyer A (1982). The behaviour of the abdominal muscles during inspiratory mechanical loading. *Respir Physiol* **50**, 63–73.

Mellen NM, Janczewski WA, Bocchiaro CM & Feldman JL (2003). Opioid-induced quantal slowing reveals dual networks for respiratory rhythm generation. *Neuron* **37**, 821–826.

Nattie E (2000). Multiple sites for central chemoreception: their roles in response sensitivity and in sleep and wakefulness. *J Respir Physiol* **122**, 223–235.

Nattie E & Li A (2010). Central chemoreception in wakefulness and sleep: evidence for a distributed network and a role for orexin. *J Appl Physiol* **108**, 1417–1424.
Nattie EE (2001). Central chemosensitivity, sleep, and wakefulness. *Respir Physiol* **129**, 257–268.
Nattie EE & Li A (2001). CO_2 dialysis in the medullary raphe of the rat increases ventilation in sleep. *J Appl Physiol* **90**, 1247–1257.
Nattie EE & Li A (2002). CO_2 dialysis in nucleus tractus solitarius region of rat increases ventilation in sleep and wakefulness. *J Appl Physiol* **92**, 2119–2130.
Oliven A, Jr, Deal EC, Kelsen SG & Cherniack NS (1985). Effects of hypercapnia on inspiratory and expiratory muscle activity during expiration. *J Appl Physiol* **59**, 1560–1565.
Pagliardini S, Greer JJ, Funk GD & Dickson CT (2012). State-dependent modulation of breathing in urethane-anesthetized rats. *J Neurosci* **32**, 11259–11270.
Pagliardini S, Janczewski WA, Tan WB, Dickson CT, Deisseroth K & Feldman JL (2011). Active expiration induced by excitation of ventral medulla in adult anesthetized rats. *J Neurosci* **31**, 2895–2905.
Praud JP, Allest AMD & Nedelcoux H (1989). Sleep-related abdominal muscle behavior during partial or complete obstructed breathing in prepubertal children. *Pediatr Res* **26**, 347–350.
Sherrey JH & Megirian D (1977). State dependence of upper airway respiratory motoneurons: functions of the cricothyroid and nasolabial muscles of the unanesthetized rat. *Electroencephalogr Clin Neurophysiol* **43**, 218–228.
Sherrey JH & Megirian D (1980). Respiratory EMG activity of the posterior cricoarythenoid, cricothyroid and diaphragm muscles during sleep. *Respir Physiol* **39**, 355–365.
Sherrey JH, Pollard MJ & Megirian D (1988). Proprioceptive, chemoreceptive and sleep state modulation of expiratory muscle activity in the rat. *Exp Neurol* **101**, 50–62.
da Silva GSF, Giusti H, Benedetti M, Dias MB, Gargaglioni LH, Branco LGS & Glass ML (2011). Serotonergic neurons in the nucleus raphe obscurus contribute to interaction between central and peripheral ventilatory responses to hypercapnia. *Pflugers Arch* **462**, 407–418.
da Silva GSF, Giusti H, Castro OW, Garcia-Cairasco N, Gargaglioni LH, Branco LGS & Glass ML (2013). Serotonergic neurons in the nucleus raphé obscurus are not involved in the ventilatory and thermoregulatory responses to hypoxia in adult rats. *Respir Physiol Neurobiol* **187**, 139–148.
da Silva GSF, Li A & Nattie E (2010). High CO_2/H^+ dialysis in the caudal ventrolateral medulla (Loeschcke's area) increases ventilation in wakefulness. *Respir Physiol Neurobiol* **171**, 46–53.
Smith CA, Ainsworth DM, Henderson KS & Dempsey JA (1989). Differential responses of expiratory muscles to chemical stimuli in awake dogs. *J Appl Physiol* **66**, 384–391.
Smith CA, Ainsworth DM, Henderson KS & Dempsey JA (1990). The influence of carotid body chemoreceptors on expiratory muscle activity. *Respir Physiol* **82**, 123–136.
Takasaki Y, Orr D, Popkin J, Xie AL & Bradley TD (1989). Effect of hypercapnia and hypoxia on respiratory muscle activation in humans. *J Appl Physiol* **67**, 1776–1784.
Taylor NC, Li A & Nattie EE (2006). Ventilatory effects of muscimol microdialysis into the rostral medullary raphé region of conscious rats. *Respir Physiol Neurobiol* **153**, 203–216.
De Troyer A, Gilmartin JJ & Ninane V (1989). Abdominal muscle use during breathing in unanesthetized dogs. *J Appl Physiol* **66**, 20–27.
Vicente MC, Dias MB, Fonseca EM, Bícego KC & Gargaglioni LH (2016). Orexinergic system in the locus coeruleus modulates the CO_2 ventilatory response. *Pflügers Arch* **468**, 763–774.
Wakai Y, Welsh MM, Leevers AM & Road JD (1992). Expiratory muscle activity in the awake and sleeping human during lung inflation and hypercapnia. *J Appl Physiol* **72**, 881–887.

Additional information

Competing interests

The authors declare no competing interests.

Author contributions

I.P.L. and C.A.S. contributed equally to acquisition, analysis, interpretation of data and manuscript revision; L.H.G. contributed to the design of the work and manuscript revision; G.S.F.S contributed to acquisition, analysis and interpretation of data, conception, study design, drafting and manuscript revision. All authors revised and approved the final version of the manuscript.

Funding

This study was funded by Sao Paulo Research Foundation (FAPESP): Young Investigator Award (Grant nos. 2013/17606-9 and 2014/12190-1) and undergraduate scholarships (2016/11061-9 and 2015/04926-0).

Acknowledgments

We thank Dr Bill Milsom and Dr Daniel Zoccal for kindly reading the manuscript, for suggesting improvements, and for their insightful discussions and comments. We would also like to thank Dr Lynn Hartzler for her kind help with grammatical corrections in the final version.